

International Atomic Energy Agency

INDC(TAI)-002/GI

INT(83)-1

---

**INDC**

**INTERNATIONAL NUCLEAR DATA COMMITTEE**

---

Instrumentation for a Fast Neutron

Time-of-Flight Spectrometer

by

G.G. Hoyes, T. Vilaithong and N. Chirapatpimol  
Department of Physics  
Chiang Mai University  
Thailand

This work has been performed under IAEA  
Technical Co-operation Interregional Project INT/1/018



November 1982

---

**IAEA NUCLEAR DATA SECTION, WAGRAMERSTRASSE 5, A-1400 VIENNA**

Reproduced by the IAEA in Austria  
March 1983  
83-1869

Instrumentation for a Fast Neutron

Time-of-Flight Spectrometer

by

G.G. Hoyes, T. Vilaithong and N. Chirapatpimol  
Department of Physics  
Chiang Mai University  
Thailand

This work has been performed under IAEA  
Technical Co-operation Interregional Project INT/1/018

November 1982

# INSTRUMENTATION FOR A FAST NEUTRON TIME OF FLIGHT SPECTROMETER.\*

G.G.HOYES, T.VILAITHONG, N.CHIRAPATPIMOL.

Department of Physics, Chiang Mai University, Thailand.

A system of fast electronic NIM modules for a neutron time-of-flight (TOF) spectrometer has been developed. The required specifications of the modules are discussed. Practical problems met during construction and some test results of the modules are presented. The system is being used routinely in the measurement of fast neutron spectra using the time-of-flight technique. The feasibility of building our own system of fast electronics for a fast neutron spectrometer is thus demonstrated.

\* This work was supported in part by the National Research Council.

## 1. Introduction.

Our objective in this work was to build a neutron time-of-flight (TOF) spectrometer of comparable resolution to those possessed by other laboratories for use in the new Neutron Physics Laboratory to be established in 1983, and so to acquire the facilities to do high resolution TOF measurements. Our aim therefore was not to improve on the performance of existing spectrometers but to produce a state-of-the-art TOF spectrometer as soon as possible with limited funds. Because of the limited funds it became obvious that we would have to build most of the necessary electronic modules which we did not already possess and purchase only those items which we could not produce i.e. scintillators, photomultiplier tubes etc. Included amongst the modules we have built ourselves are a dual constant fraction discriminator (CFD), a fast linear gate and stretcher (LGS), a linear fan out (LFO), a pulse shape discriminator (PSD) and tube bases.

### 1.1 Principle.

The kinetic energy of a fast neutron is usually measured by means of the time-of-flight technique in which the time,  $t_n$  it takes a neutron to travel a fixed distance,  $l$  is measured. The time-of-flight is related to energy  $E_n$  by the equation

$$E_n = E_0 \left[ \left( 1 - \frac{l^2}{t_n^2 c^2} \right)^{-1/2} - 1 \right] \dots\dots\dots 1)$$

where  $E_0$  is the rest mass of the neutron and  $c$  the speed of light. Thus  $E_n$  is related to the flight time per meter  $t_n/l$  as shown in table 1. (1)

<u><math>E_n</math> (MeV)</u>	<u><math>t_n/l</math> (ns/m)</u>
1	72.355
5	32.461
10	23.044
100	7.795

Table 1.  $t_n/l$  for various energies.

In our spectrometer we use a flight path of the order of two meters and our sources are a 14MeV neutron generator and a Am-Be

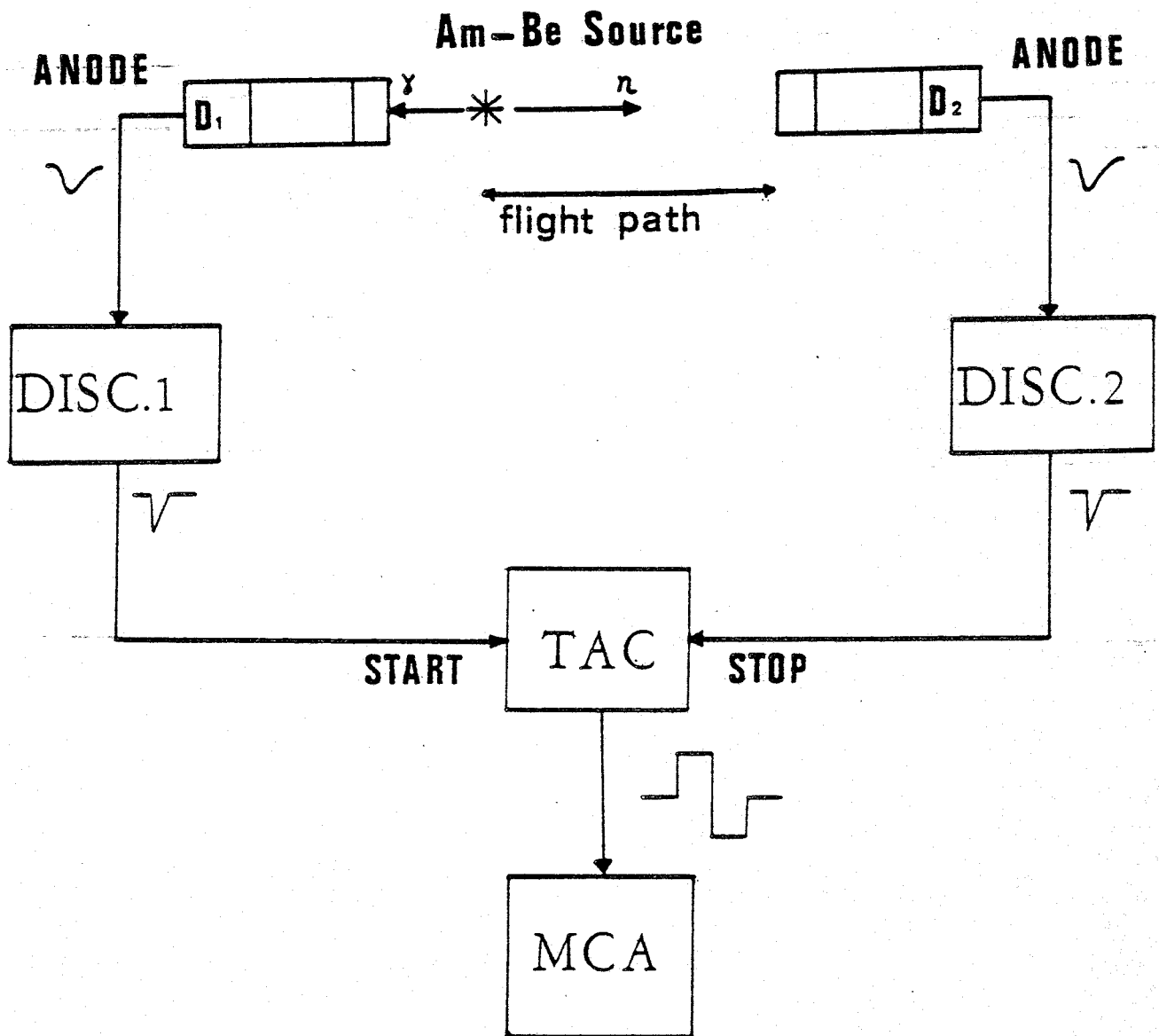


Fig.1. Basic time-of-flight spectrometer.

source with peaks at 3.2 and 4.8 MeV.

Fig.1. shows a basic TOF electronic circuit using the associated gamma ray technique. The gamma ray associated with the emission of a neutron is detected by D1. The linear anode signal from D1 is fed to a discriminator which produces a precise timing signal at the start of the flight time. This signal starts the time to amplitude converter (TAC). When the neutron arrives at detector D2 a similar signal is developed representing the end of the flight time and this stops the TAC. Thus the amplitude of the TAC output is linearly proportional to the time-of-flight of the neutron. Feeding the TAC output to an MCA will produce a spectrum representing the energy distribution of neutrons emitted by the source.

### 1.2. Uncorrelated signals and random coincidence.

The main problem with this simple circuit is that of uncorrelated signals which increase the dead time of the TAC. Uncorrelated signals from the source as well as scattered and background radiation can be reduced by using a fast coincidence circuit to gate the TAC. But random coincidence can still occur within the resolving time of the coincidence circuit, particularly due to the high gamma radiation usually associated with neutron sources falling on detector D2. This problem is solved by the inclusion of a neutron-gamma pulse shape discriminator in the D2 branch to reject gamma pulses. These additions are shown in the complete neutron t.o.f. circuit in fig.2.

## 2. Neutron TOF spectrometer.

The most important parameter in the electronic system is the time resolution. The state-of-the-art at present in such systems is typically less than 1ns and this is what we aim for. Fast scintillators and tubes were used for this purpose. The bases, CFD, LFO, and PSD, were built by ourselves as was the LGS shown later.

### 2.1 Tube bases.

The tube base circuit was based on that of the Ortec 265 which was designed for use with the RCA 8575 PMT for use in fast timing applications, whilst retaining good energy resolution.

Fig.3. shows the base circuit. The fast anode output is used for timing. The risetime of the signal should be as short as possible, typically about 3ns depending on the PMT and scintillator characteristics. We found that at high count rates (>about 30 KHz) and high current pulse amplitudes (about 0.5A)

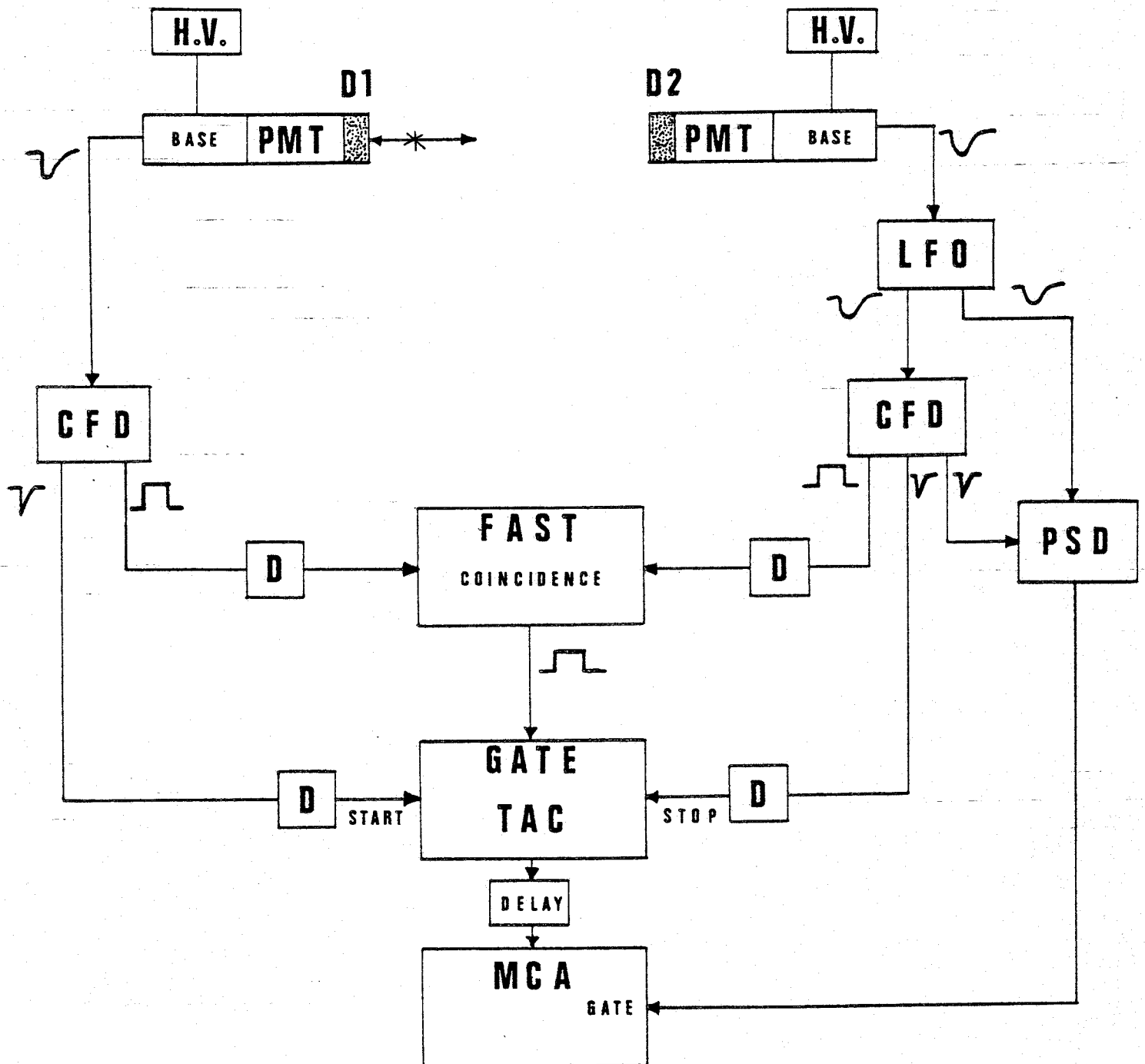
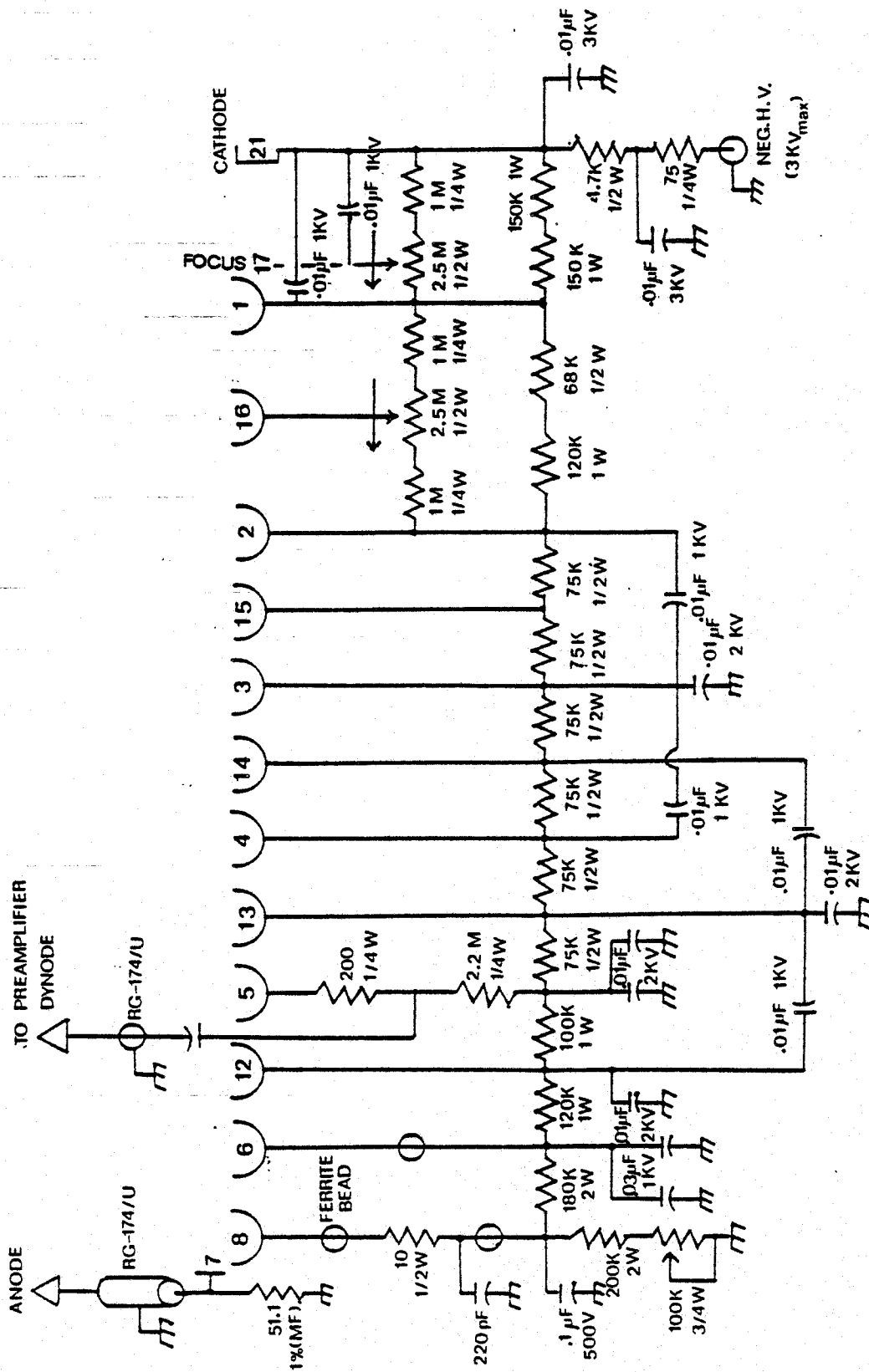


Fig. 2 Complete neutron t.o.f. spectrometer : LFO-linear fan out, CFD-constant fraction discriminator, PSD-pulse shape discriminator, TAC-time to amplitude converter, D-delay, MCA-multichannel analyser.





**Fig. 3. Tube Base Circuit.**

extra stabilizing capacitors were needed on the last four dynodes as shown. The 51.1 ohm resistor at the anode, as well as back terminating the output coaxial cable, which may be quite long, also halves the output voltage amplitude so that the signal height is compatible with the CFD input (5v).

## 2.2 Constant fraction discriminator.

Probably the most important unit of the spectrometer as far as time resolution is concerned is the time pick off or discriminator. This is the unit which must generate a precise timing signal at its output as independent as possible of the amplitude of the linear input signal from the PMT anode. This is known as the time walk of the pick off and should be a minimum. Time jitter is a variation in the timing of the output signal due to noise on the input waveshape. These two effects are illustrated in fig.4a and 4b.

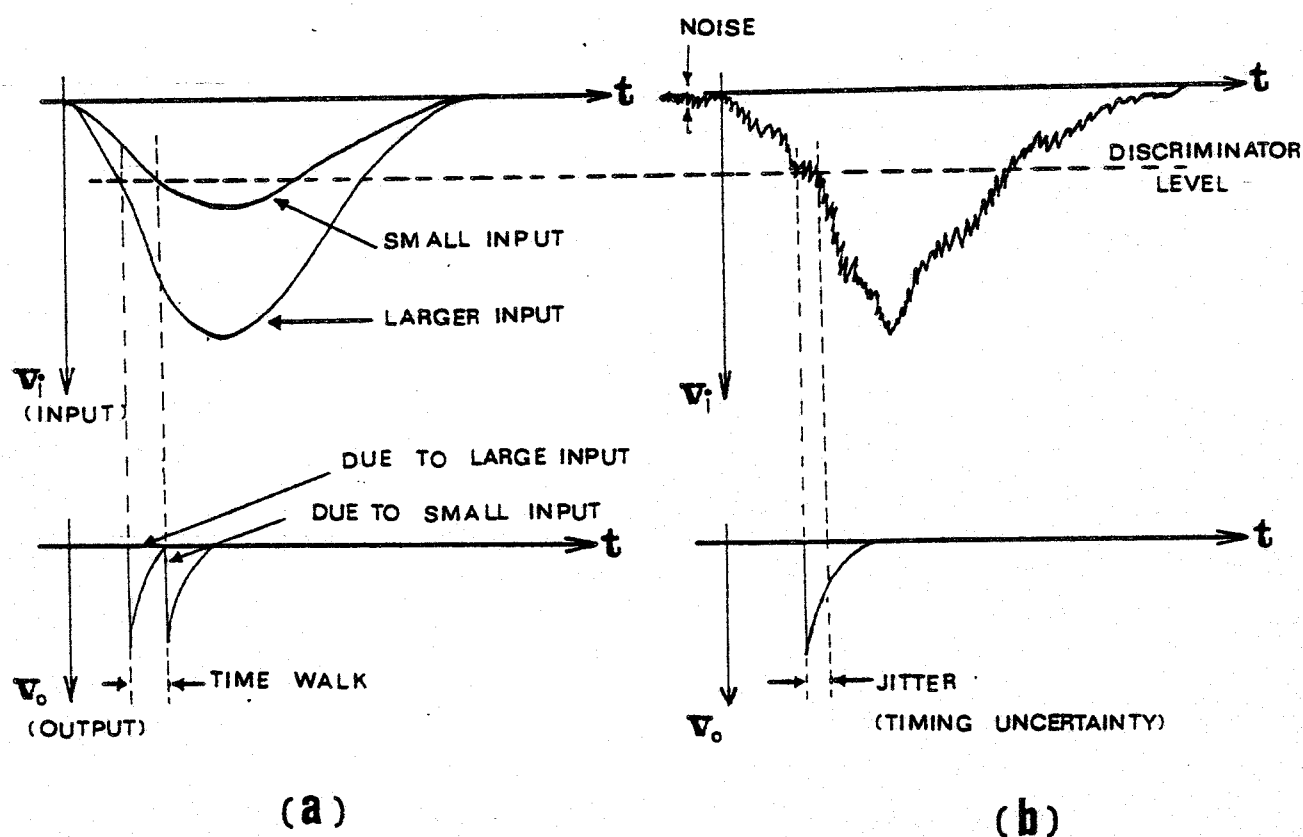


Fig.4. Showing the effect of time walk (a) and jitter (b) on the output of the discriminator.

Time jitter is minimised by setting the discriminator threshold to give an output at the time of maximum slope of the leading edge of the input signal. This has been shown by many workers (2,3) to occur at 10-30% of maximum pulse height for most fast scintillators.

Time walk is minimised by keeping the discriminator level at this optimum fraction of pulse height, independent of the absolute height of the input anode signal. These two concepts are combined in the constant fraction of pulse height trigger CFPT or constant fraction discriminator CFD as it is more well known (2,3). The CFD gives superior timing performance to the other types of time pick offs (e.g. leading edge, and zero cross) particularly when a large dynamic range of input signals is required. For a total system timing performance of less than one nanosecond, the individual contribution of any one unit must be much less than this. Typical walk values for a CFD are less than 200ps for a 100:1 dynamic range of input signals.

Fig.5a shows the block diagram of our CFD, based on a design by Pouthas and Engrand (4). The constant fraction of pulse height for the discriminator is set by the input resistors at  $R1/(R1+R2) = 17.5\%$ , although this value is not critical. The principle of how the CFD works is shown in fig.5b. The input signal (A) is delayed and inverted (B) and added to a fixed fraction (C) of the input signal to produce a bipolar pulse (B+C) with a zero cross at the time of the input reaching 17.5% of maximum amplitude. The zero cross is detected by comparator 1 and causes the D flip flop to give an output (D) for 8ns, provided that the D input has previously been armed by comparator 2 which acts as a pulse height discriminator. Our circuit has both positive and negative NIM outputs as well as input diode protection of the comparators. The threshold setting is variable from zero to four volts but this range can easily be changed. The threshold potentiometer has a ten turn dial to enable calibration of the discriminator in terms of energy of the input pulse, using the fast linear gate and stretcher described later.

Two of these circuits were built into one standard width NIM module, the delay and invert cable being connected externally to allow for optimum choice of delay to suit the detector used. Due to the high switching speed of the ECL circuits used, one side of a double sided printed circuit board was used as a ground plane and a compact design layout of components was used to minimise unwanted reflections and delays respectively. See appendix 1 for the complete circuit used.

It was not possible to measure the absolute value of walk introduced by each of the CFD's due to the lack of high speed test instrumentation and only the total system time resolution could be used to indicate their correct operation.

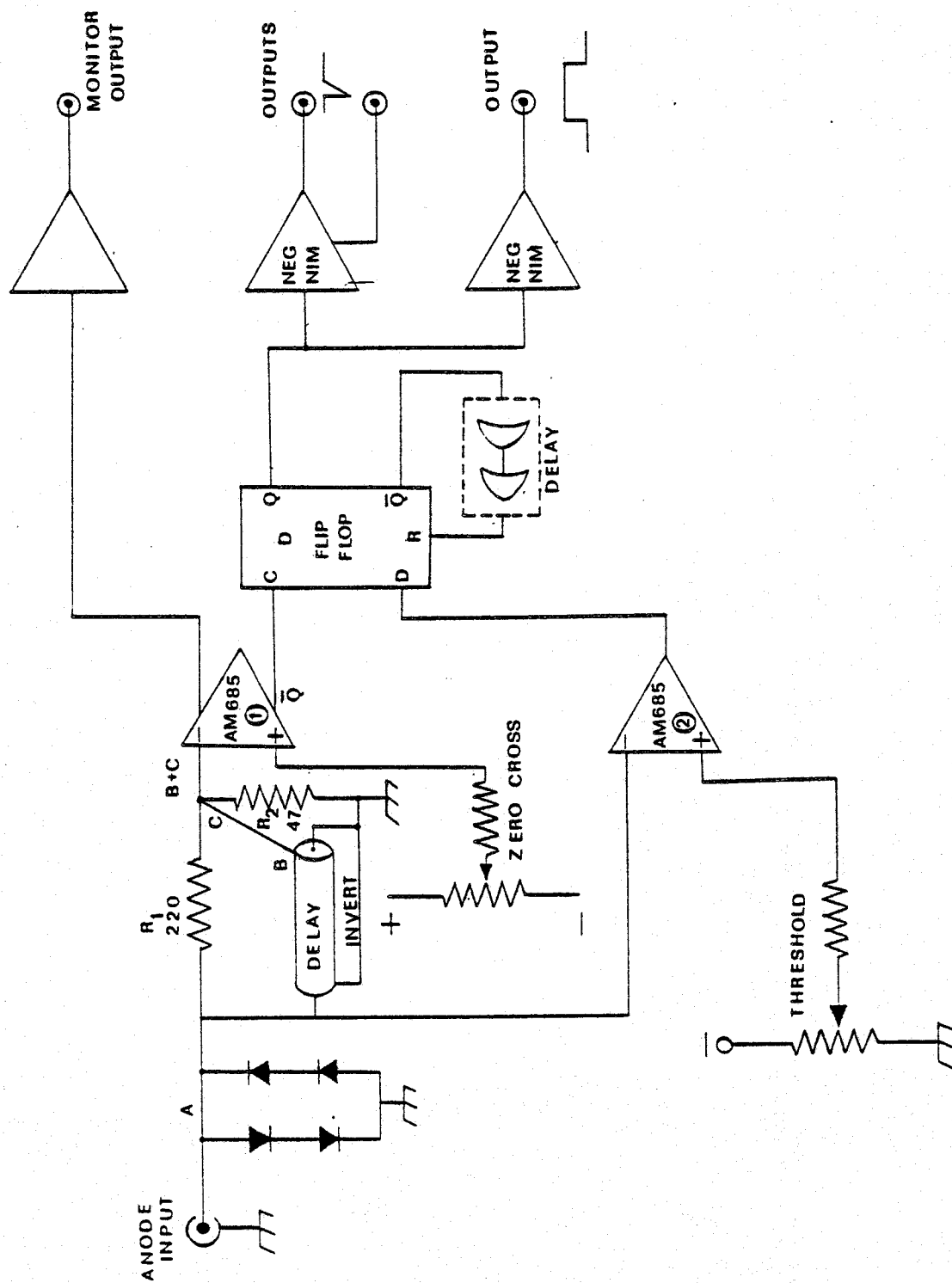


Fig.5. (a) Constant fraction discriminator block diagram.

(b) Principle of operation.

### 2.3 Linear fan out.

The linear fan out module (5) comprises an emitter follower feeding two more emitter followers to produce two active outputs and one direct output. This circuit uses high speed transistors to obtain the wide bandwidth necessary for undistorted reproduction of the fast anode input signal. We built two such circuits into one single width NIM module.

### 2.4 Pulse shape discriminator.

The pulse shape discriminator circuit (PSD) distinguishes between neutrons and gamma pulses received by D2 and is needed to remove such true coincidences as may occur when a neutron is received by D1 and a gamma ray is received by D2. It is also needed to eliminate accidental coincidences from gamma background radiation incident on D2.

The PSD must be able to distinguish between the different shapes of pulses due to neutrons and gamma rays incident on the NE213 scintillator. It must be able to utilize the fast negative linear anode pulse rather than the slower dynode signal so that the dead time of the spectrometer is not made too high. Because of the fast rise time of the anode signal (3ns), high speed circuit techniques, i.e. ground planes, terminated transmission lines, adequate decoupling etc., must be used. For general purpose use both fast negative and slow positive logic outputs would be desirable.

The PSD circuit used is shown in block diagram form in fig.6 and can be conveniently divided into two parts: the linear pulse shaping preamplifier which distinguishes between neutron and gamma pulse shapes, and the ECL logic circuit which provides logic outputs for neutron, gamma, and neutron OR gamma signals. The preamplifier is based on a design by Speer et al. (6) and incorporates modifications proposed by Biakowski and Szezepankowski (7). The ECL circuitry has been redesigned by us to use more recent types of ECL IC's. All the gates are the same type (NOR) for convenience of building, testing and component ordering. In addition all of our logic outputs are in prompt time coincidence. The complete diagram of the PSD is shown in appendix 2. For more details and information on construction see ref. 8).

Fig. 7 shows some test results on the preamplifier section of the PSD using the test circuit of fig. 8. These show a clear separation between the neutron and gamma events, : 21ns between peaks (scale:0.5ns/channel). See ref.8) for a more complete treatment of the test data.

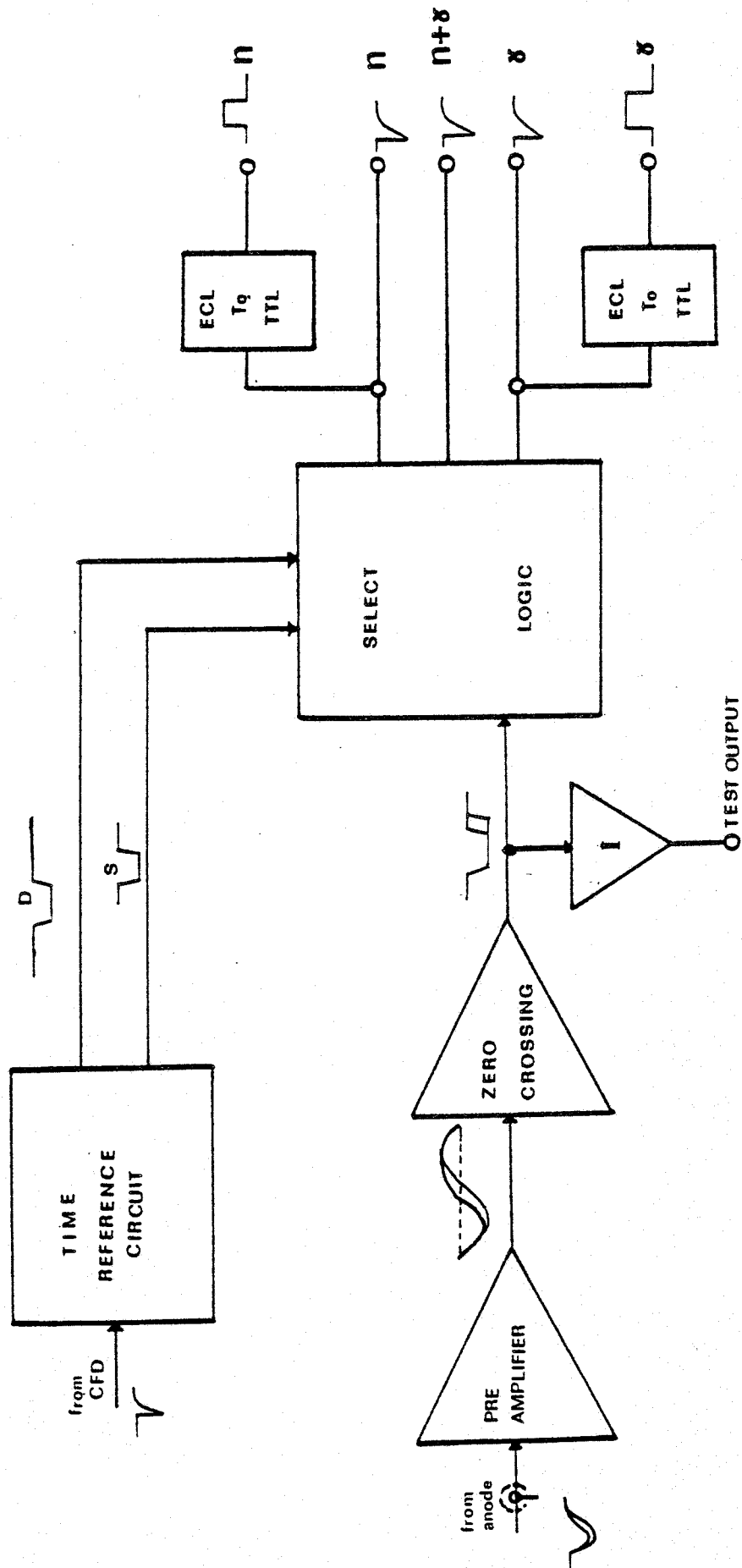


Fig. 6. Pulse shape discriminator block diagram.

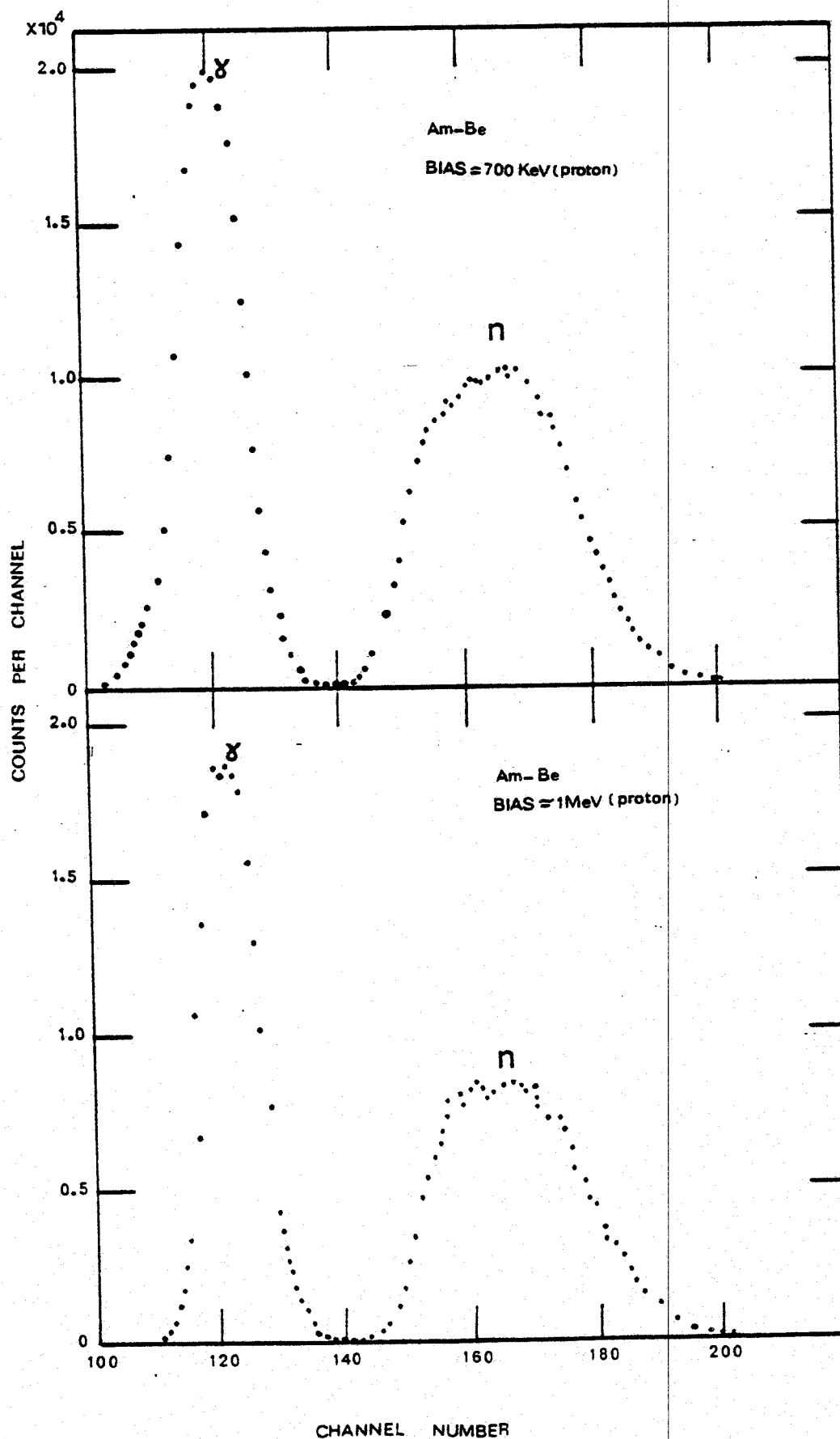


Fig.7. P.S.D. test:neutron-gamma separation using an AmBe source (0.5ns/channel)

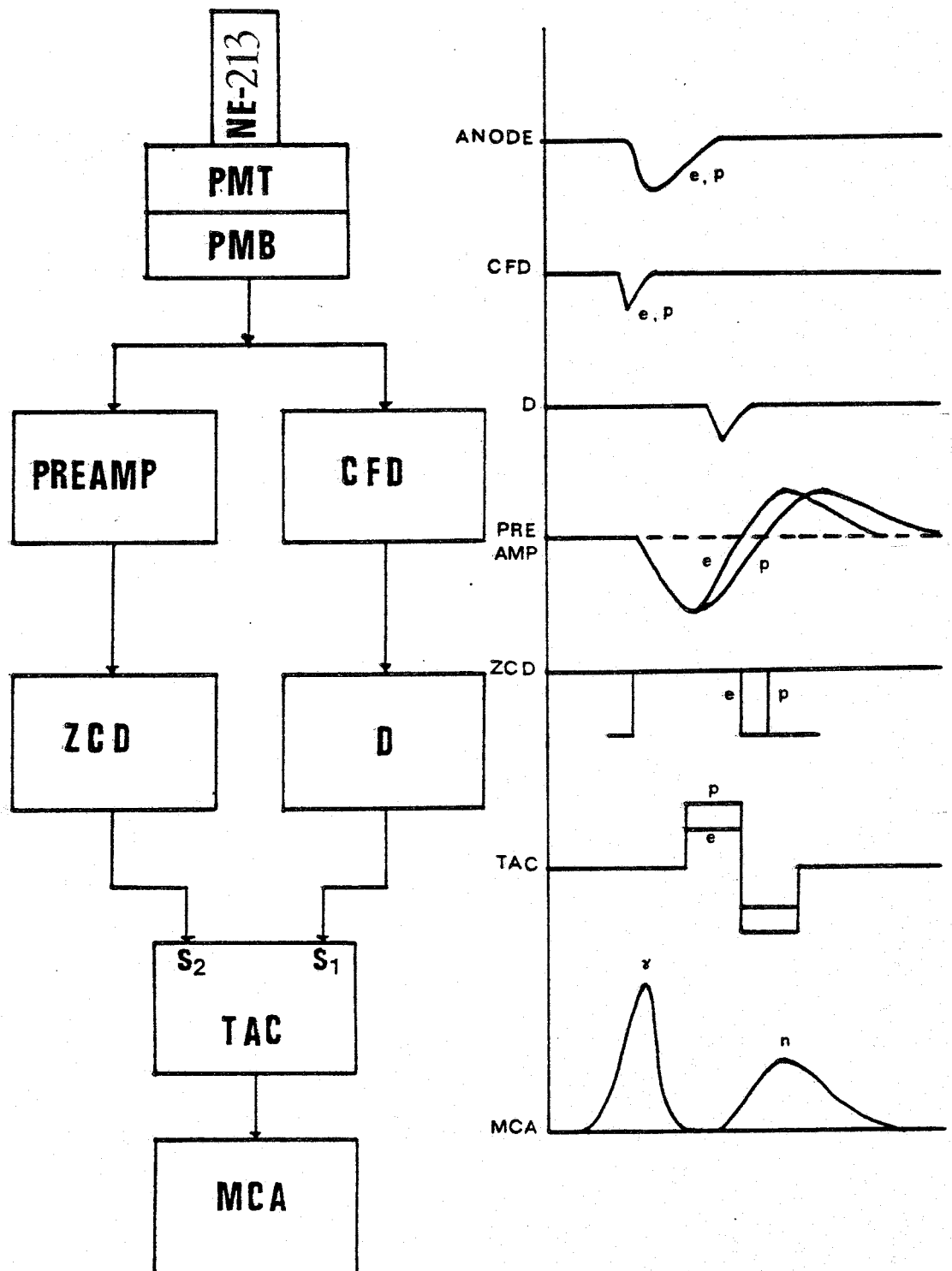


Fig.8. P.S.D. test circuit with waveshapes.



## 2.5 Fast linear gate and stretcher.

As mentioned earlier the CFD was energy calibrated using a linear gate and stretcher circuit (LGS). The calibration circuit is shown in fig. 9. The threshold control on the CFD was used to select the minimum energy level gated by the LGS. Thus if the MCA shows peaks from known energy sources the threshold control can be calibrated by adjusting the threshold level to coincide with each of these peaks on the MCA display.

The block diagram of the LGS is shown in fig. 10. A detailed circuit is given in appendix 3. This circuit was based on a design by Baldwin (9) the trigger select and gate control circuits being slightly modified to use all the same type of ECL NOR gates (MC10102). The discrete inverting output operational amplifier of the original design was replaced with an integrated circuit stage after experiencing thermal drift problems with the discrete design.

The LGS allows for a fast linear anode signal to be gated by a fast NIM logic pulse (A, B, or A OR B) and then stretched and inverted so that the output is compatible with most of the inputs of MCA's.

The fast linear gate and stretcher as the name implies consists of two main circuits:- a fast gate for gating the anode signal from the photomultiplier tube, and a stretcher to make the output from the gate wide enough to be accepted by an MCA.

The gate circuit is composed of the input amplifier, the gate trigger selector, and the gate control circuits. When the gate mode switch is in the open position all input pulses are passed onto the stretcher circuit. In the closed position no signals are allowed to pass. In the triggered position only those input pulses which have an associated trigger input pulse will be passed. Either the A or the B or both trigger inputs can be used to control the gate by means of the trigger select switch circuit. The trigger inputs are typically derived from the fast logic outputs of fast discriminators, such as CFD's, fed by the same linear input as the LGS. The trigger inputs are thus too narrow to gate the linear signal directly and must be widened. This is the function of the gate control circuit which produces one variable width output pulse for each trigger pulse. The linear input signal must lie within the time duration of the gate control signal and the gate width monitor is provided to compare the timing of the two so that the correct amount of delay can be inserted in the linear input line and the gate width can be adjusted. A portion of the gate control output is also fed back to the input as a gate precharge to assist the gate in turning on just as the linear input signal arrives. This is particularly important for linear operation with small signals.

The stretcher circuit, delay and output amplifier are of conventional design. In the stretcher the charge of the input is converted to a voltage by means of an integrating capacitor. A buffer is included to prevent subsequent circuits loading this capacitor. The one microsecond delay line is included for convenience as it is often necessary to delay the output. The

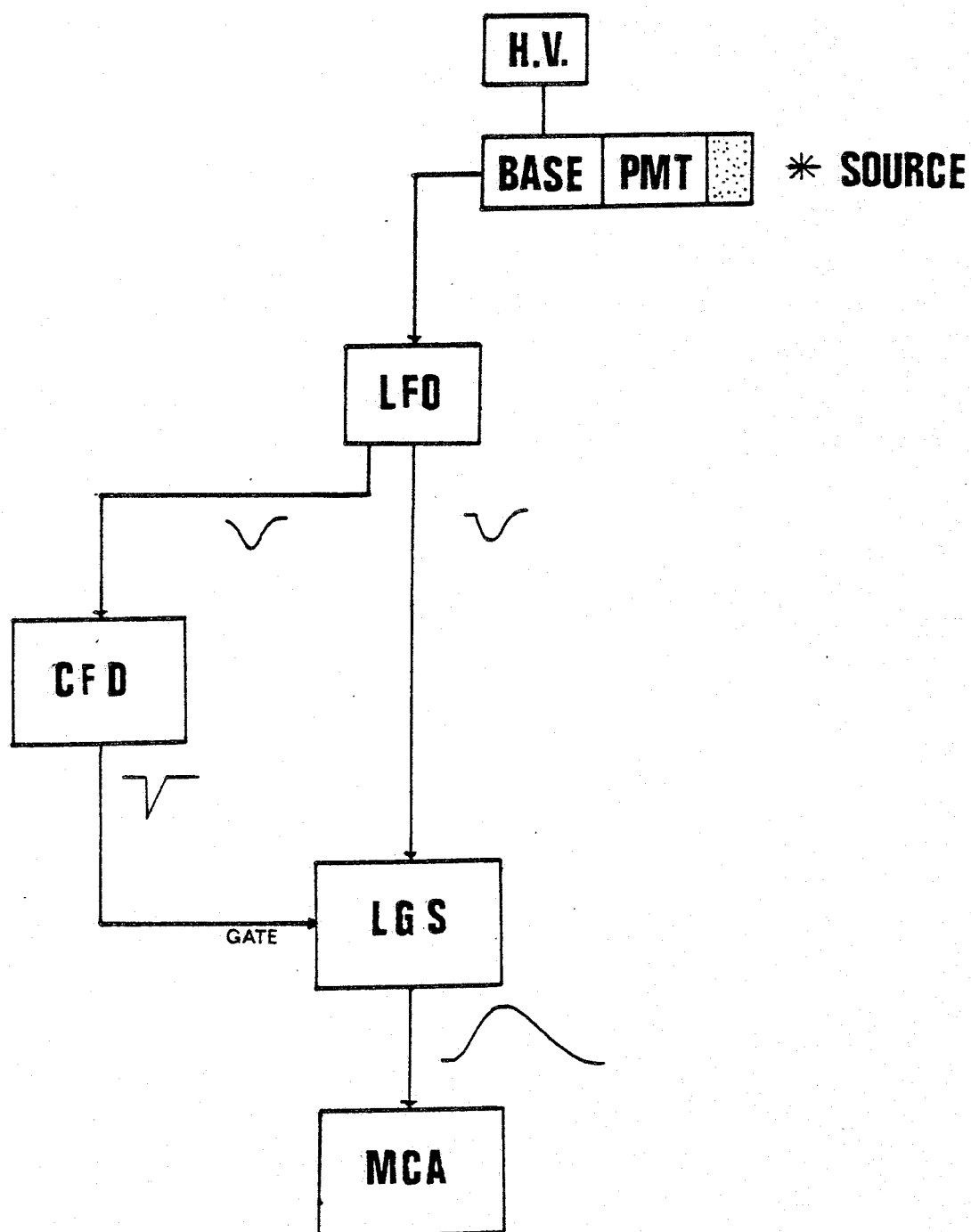


Fig.9. Energy calibration of CFD using LGS.

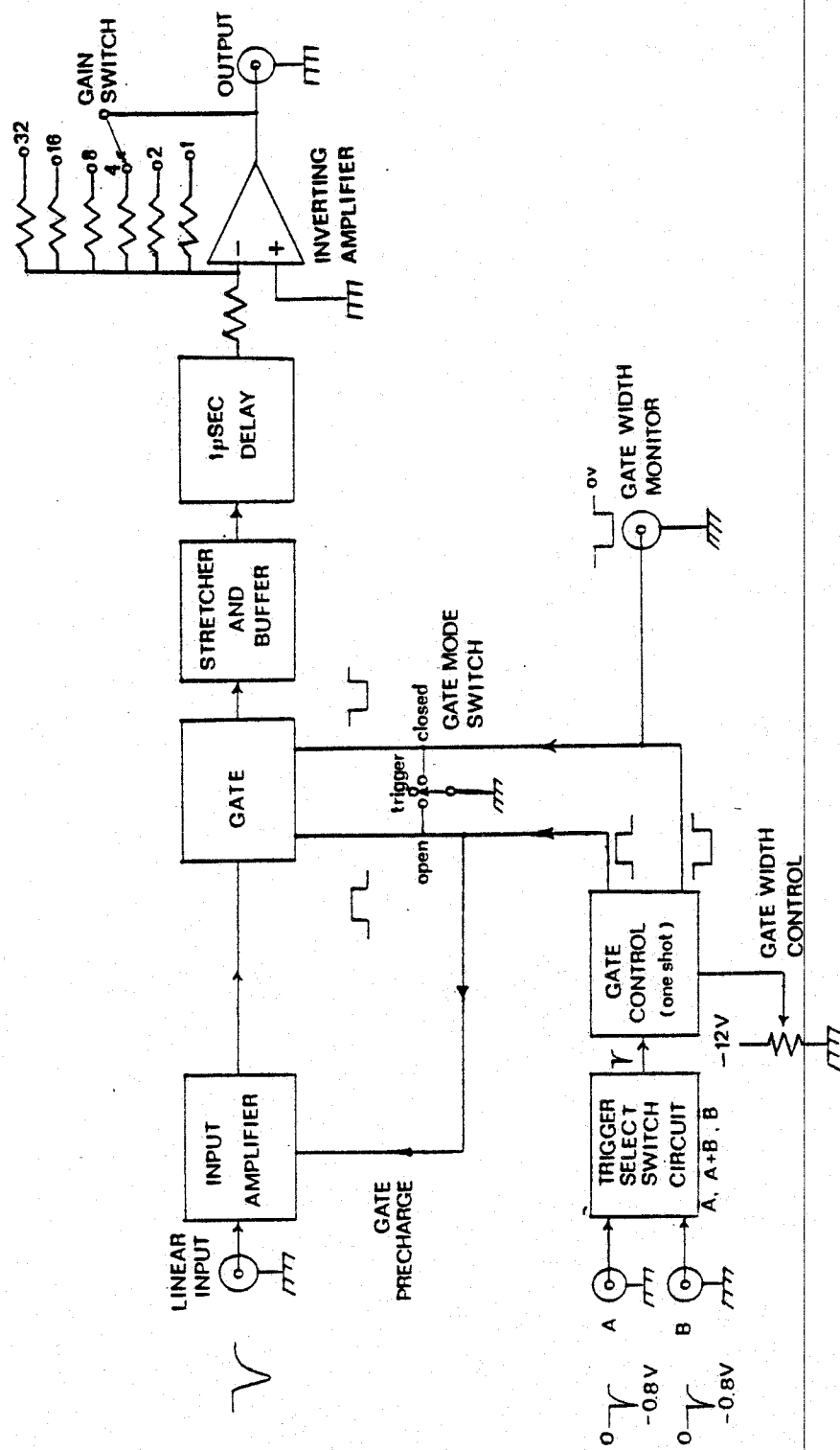


Fig.10. Fast linear gate and stretcher.

output amplifier provides a means of adjusting the output amplitude via the gain control, and inverts the signal to give a positive polarity compatible with the MCA input.

## 2.6 Time resolution.

The final spectrometer circuit of fig.2 uses the modules constructed. The fast coincidence is an Ortec 414A, the TAC is a Canberra 2044, and the MCA used is an Ortec 6220. Fig. 11 shows the intrinsic time resolution of the complete spectrometer as displayed on the MCA screen. It can be seen that for a system composed of two 2in x 2in scintillators we have achieved a time resolution at FWHM of 0.78ns, well within the target of less than 1ns.

## 3. Problems encountered during construction.

The acquisition of components for building some of these modules presented some problems. Due to the high speed of the modules, integrated circuits, transistors, etc. having a wide bandwidth were required, often of the type which are not common even in their countries of origin, and are relatively expensive. Addresses of suppliers and assistance in finding such components can be given on request.

It should be mentioned here that the expenditure on instrumentation in this project was cut drastically by undertaking construction ourselves, particularly for the simpler circuits such as tube bases where the savings approached 80% of the commercial cost.

All the modules described were contained in single width NIM modules of our own make. The NIM bins and MCA were all contained in a 19" rack. Drawings for the NIM modules and rack as well as for the PCB layouts and circuits themselves are all available on request.

## 4. Conclusion.

It can be seen then that even with the inconveniences of being distant from the major suppliers of fast electronic components and instrumentation it is possible to build a neutron time-of-flight spectrometer of high resolution. Furthermore undertaking the development of our own instrumentation enables us to gain the necessary experience to become independent of outside service calls or return to manufacturer repairs with all the associated costs and delays.

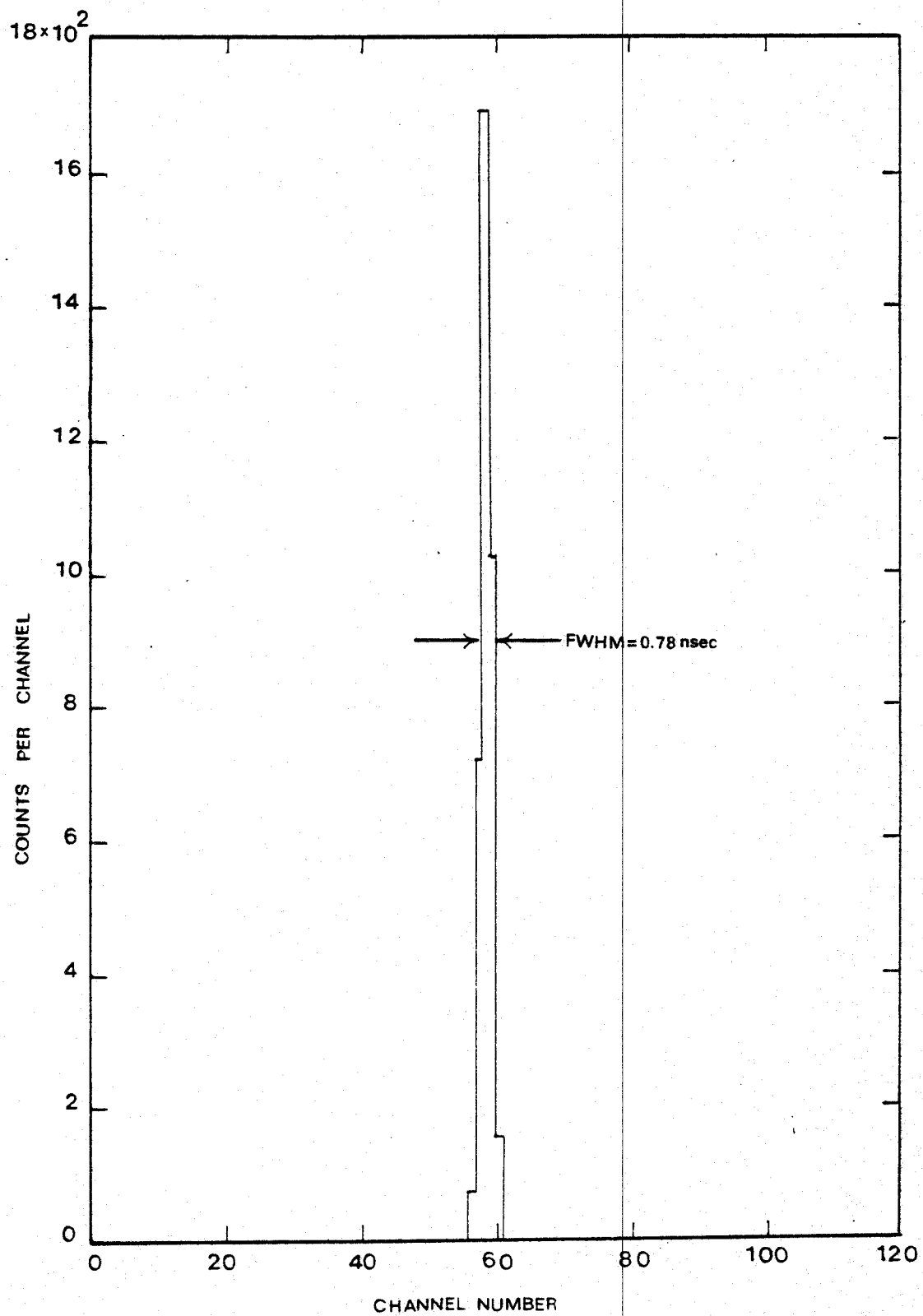
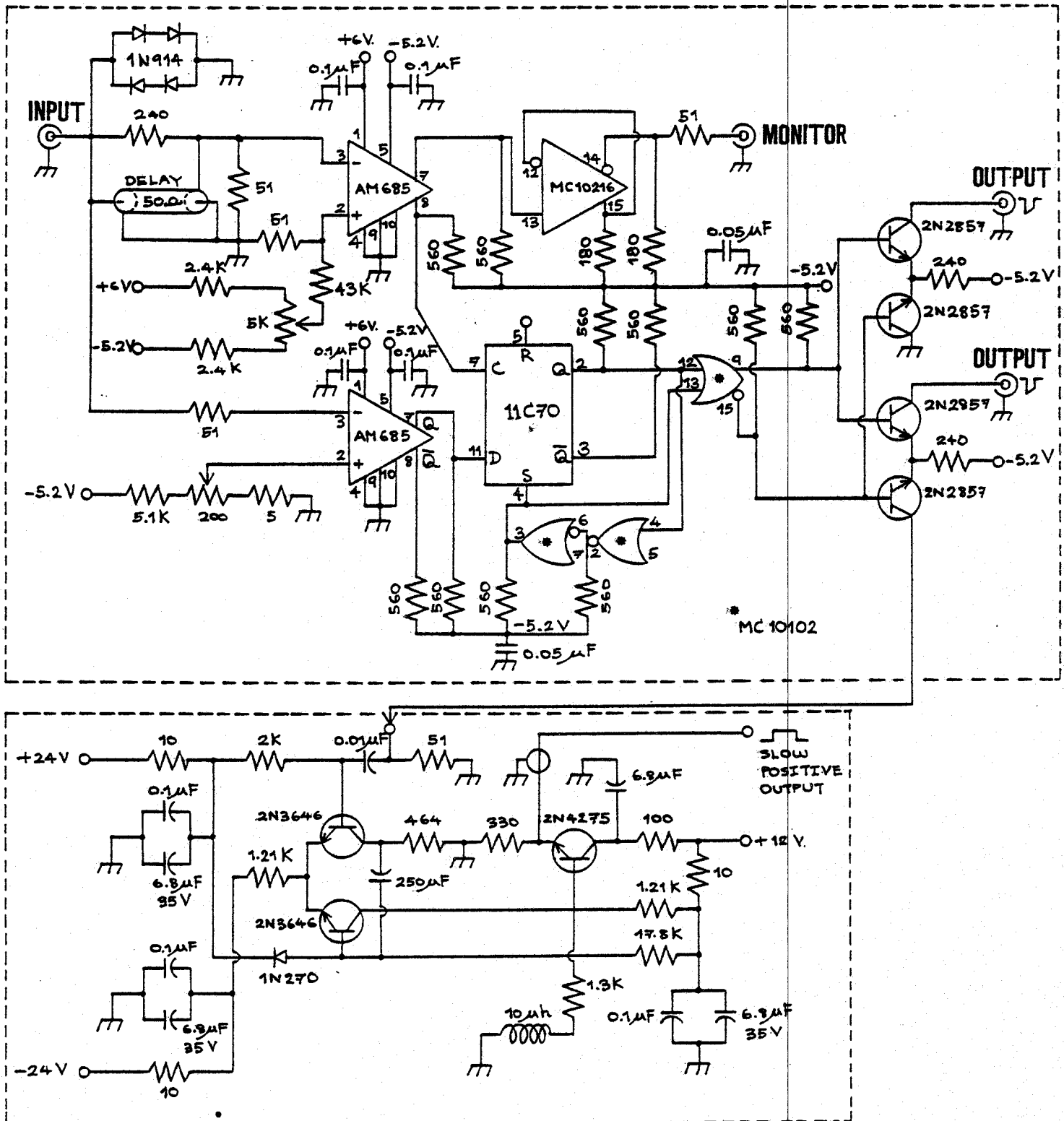


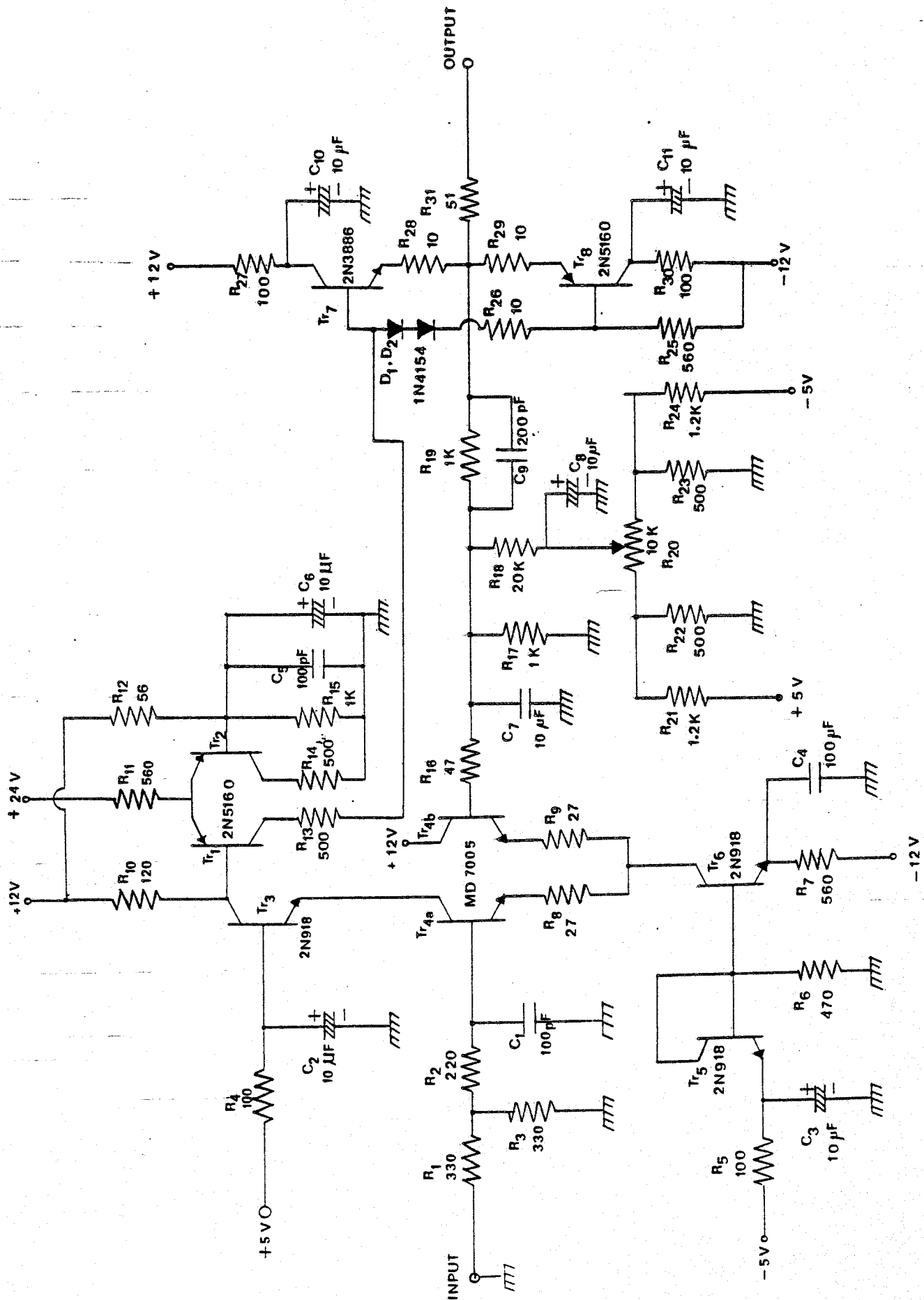
Fig.11. Intrinsic time resolution of the spectrometer.

## Appendix.

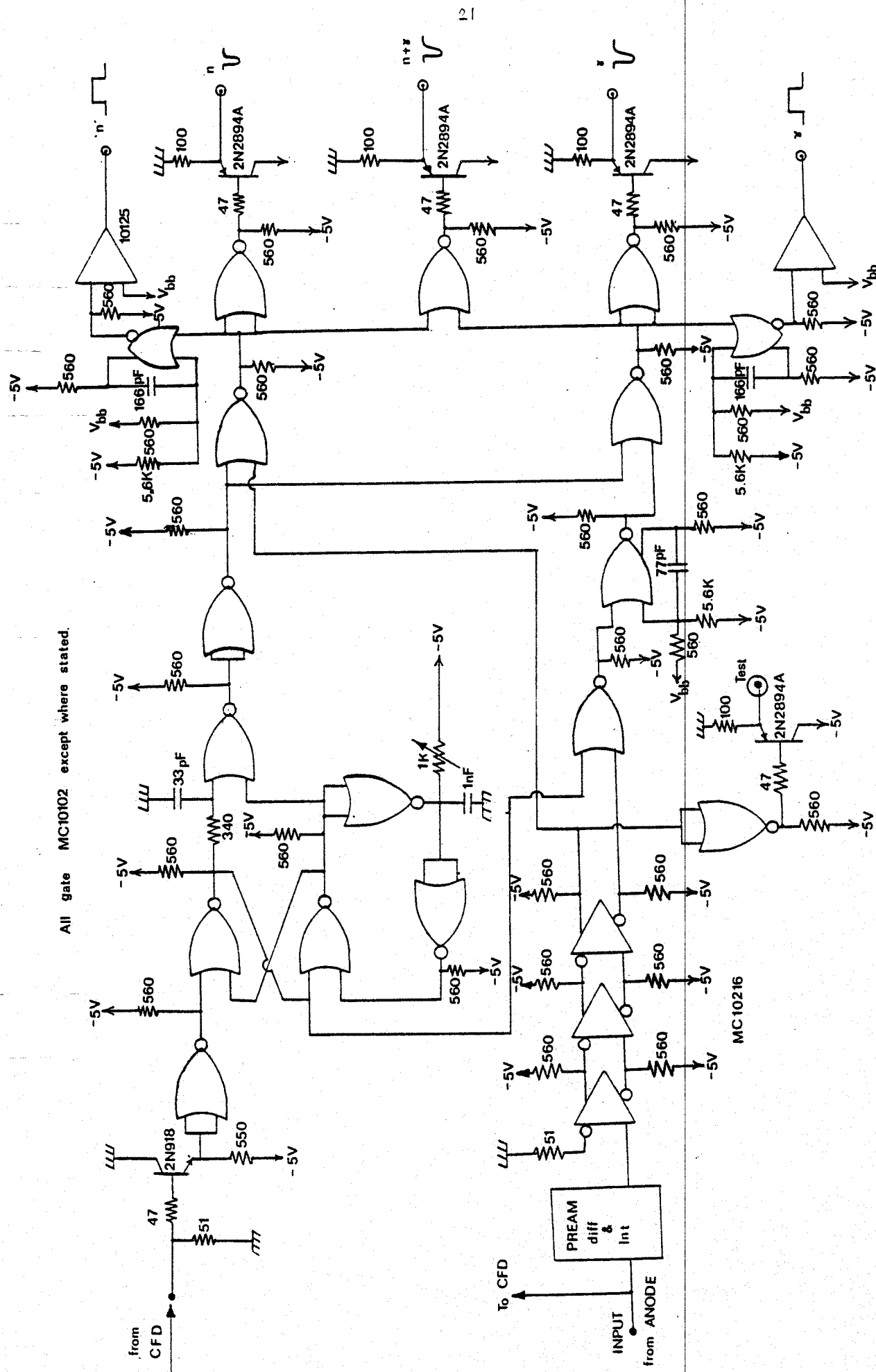
1. Constant fraction discriminator circuit.
2. Pulse shape discriminator preamplifier and logic circuit.
3. Fast linear gate and stretcher circuit.



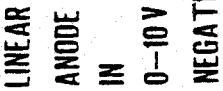
Constant Fraction Discriminator.







Pulse Shape Discriminator: Logic circuit.



## Fast Linear Gate and Stretcher: Gate Circuit



## References.

- 1) W.K.Firk, Nucl. Inst. and Meth. 162(1979)539.
- 2) D.A.Gedcke and W.J.McDonald, Nucl. Inst. and Meth. 58(1967)253.
- 3) M.R.Maier and P.Sperr, Nucl. Inst. and Meth. 87(1970)13.
- 4) J.Pouthas and M.Engrand, Nucl. Inst. and Meth. 161(1979)331.
- 5) R.Madey, F.M.Waterman, A.R.Baldwin, Nucl. Inst. and Meth. 133(1976)61
- 6) P.Sperr, H.Spieler, , M.R.Maier and D.Evers, Nucl. Inst. and Meth. 116(1974)55.
- 7) J.Bialkowski and J.Szezepankowski, Nucl. Inst. and Meth. 152(1978)589.
- 8) Seree Ruangdit, M.Sc. Thesis (Chieng Mai University, 1982).
- 9) A.R.Baldwin, Department of Physics, Kent State University, private communication.